

## CRYSTAL GROWTH, IONIC CONDUCTIVITY, AND PHOTOLYSIS OF PURE AND IMPURITY-DOPED LEAD BROMIDE SINGLE CRYSTALS

by J. F. VERWEY and J. SCHOONMAN

Afdeling voor Vaste Stof Chemie, Universiteit van Utrecht, Rijnhuizen, Jutphaas, Nederland

### Synopsis

In this paper an account is given of the preparation of lead bromide single crystals undoped and doped with monovalent and trivalent cations and with oxygen.

The conductivity of these crystals has been measured in the temperature region 50–300°C. The thermal disorder appeared to be of the same Schottky type as in lead chloride. From the slopes of the conductivity curves the activation heat for the anion vacancy migration has been calculated to be  $0.29 \pm 0.04$  eV and the heat required for the formation of one set of vacancies  $1.4 \pm 0.1$  eV.

Irradiation of pure lead bromide with ultraviolet light gives a characteristic damage as is made visible by electron and optical microscopy. The increase of the optical density varies as the square root of the irradiation time.

1. *Introduction.* During the course of the investigation of the photolysis of the lead halides we prepared pure and impurity-doped single crystals of lead bromide.

In order to know the concentration, mobility, and thermodynamics of the mobile point defects we measured the electrical conductivity of these crystals. Also some details are given about the crystal preparation and further results about the photolysis.

2. *Experimental.* a. Crystal growing: Lead bromide is precipitated by pouring together aqueous solutions of lead nitrate and hydrobromic acid. The precipitate is recrystallised from aqueous solution acidified with hydrobromic acid. After drying the lead bromide powder is melted under bromine pressure in a pyrex glass apparatus as is shown in figure 1. The tube *B* is filled with lead bromide before connection to the apparatus. After evacuation the apparatus is sealed off at *G*. About 2 ml bromine is added via funnel *D* and stopcock *E* and the apparatus is sealed off at *F*. Saturation with bromine is obtained by passing a molten zone through tube *B*, or by heating the whole tube above the melting point of lead bromide (373°C). The latter procedure is the more effective to remove adsorbed and included

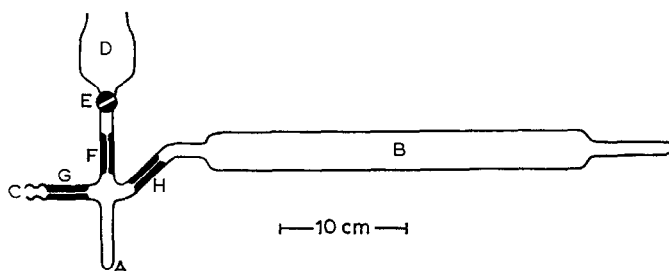


Fig. 1. Apparatus for the bromine treatment of the lead bromide melt.

A bromine container

B tube in which the lead bromide is melted

F, G, H sealing off points.

water. From a load of 200 grams of lead bromide dried first at  $120^\circ\text{C}$  for 24 hours an amount of about 1 ml water can be distilled into container A during the melting procedure. While the lead bromide is still above the melting point, water, excess bromine, and other volatile impurities are condensed by cooling container A. Then the tube B is sealed off at H. Tube B is placed in a zone refining apparatus and after 20 zone passes the clearest parts from the beginning of the tube are put into a pointed pyrex crucible, which is evacuated, sealed off and put into a Bridgman furnace. When necessary before zone refining the lead bromide melt is filtered under

TABLE I

Impurity content in lead bromide crystals (weight %) determined spectrochemically*)					
	$\text{PbBr}_2$ (pure)	$\text{PbBr}_2(\text{Tl})$	$\text{PbBr}_2(\text{Cu})$	$\text{PbBr}_2(\text{Bi})$	$\text{PbBr}_2(\text{Ag})$
Mg	0.0001	0.0004	0.0001	n.d.	0.001
Al	0.00005	0.0002	0.0001	n.d.	0.02-0
Cu	n.d.	n.d.	0.0006	n.d.	0.0001-0
Mn	n.d.	n.d.	0.0002	n.d.	
Tl	n.d.	0.01	n.d.	n.d.	
Ni	n.d.	n.d.	n.d.	n.d.	
Ag	n.d.	0.00002	n.d.		0.00005
Bi		n.d.		0.007	
Si					0.03-0
Fe	n.d.				n.d.

n.d. = not detected

\*) Thanks are due to Dr. N. W. H. Addink of the Philips Research Laboratories at Eindhoven for these analyses.

bromine pressure through a fritted glass filter to remove minute traces of solid contaminations. The results of the spectrochemical analyses of the crystals obtained, are given in table I.

Doping with copper and thallium is done by adding copper (I) bromide and thallium (I) bromide before the zone melting under vacuum. Bismuth and

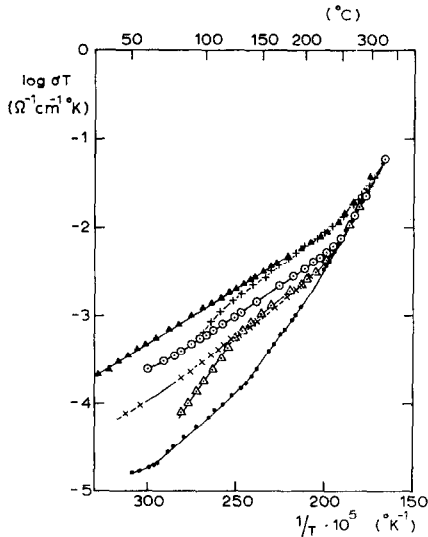


Fig. 2. Electrical conductivity,  $\sigma$ , of lead bromide plotted as  $\log \sigma T$  versus  $1/T$ .

- • • undoped lead bromide
- × × × doped with 0.002 mole % AgBr
- △ △ △ doped with about 0.002 mole % CuBr
- ○ ○ doped with 0.01 mole % TlBr
- + + + doped with PbO
- ▲ ▲ ▲ doped with 0.02 mole % TlBr.

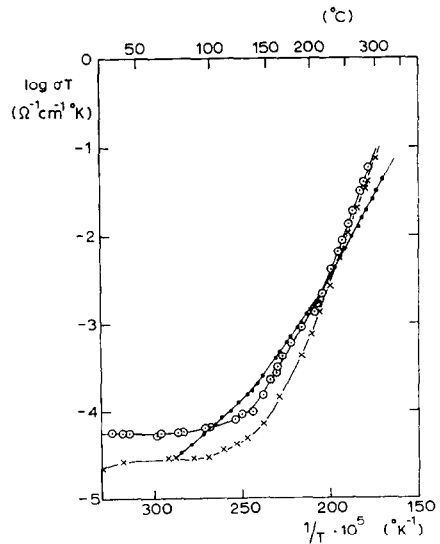


Fig. 3. Electrical conductivity,  $\sigma$ , of lead bromide plotted as  $\log \sigma T$  versus  $1/T$ .

- • • undoped lead bromide
- ○ ○ doped with 0.01 mole % BiBr<sub>3</sub>
- × × × doped with about 0.02 mole % BiBr<sub>3</sub>.

silver are introduced by placing a small amount of the metal at the beginning of the tube, followed by zone refining under bromine pressure. Incorporation of oxygen is obtained by adding lead oxide to the lead bromide.

b) Electrical conductivity: The conductivity is measured with the same impedance bridge and electrical circuit as used by De Vries<sup>1</sup>.

The bridge circuit consists of a General Radio impedance bridge (type 1608A) with external oscillator (type 1210C), used at a frequency of 1 kHz and an amplifier-null-detector (type 1232A). The crystals were cleaved perpendicular to the  $c$ -axis and the conductivity was measured as a function of increasing temperature in the region 50–300°C in a slightly modified sample holder as described by De Vries<sup>1</sup>. (More details will be published elsewhere).

3. Results. The conductivity of TlBr, CuBr, AgBr, and PbO doped crystals is shown as a function of  $T^{-1}$  in figure 2. A remarkable increase in conductivity is observed with respect to the undoped crystals. We see a decrease in conductivity after incorporation of trivalent cations, as is shown in figure 3. Compared with the solubilities of the dopants used in lead

chloride<sup>1</sup>) the solubilities of the same dopants in lead bromide are small. Therefore, it is not useful to give a quantitative treatment by isothermal plotting of the measured conductivities as a function of the incorporated dopants.

4. *Discussion.* The intrinsic point defects in lead bromide are supposed to be either of the Schottky or of the Frenkel type.

Tubandt<sup>2</sup>) *et alii* concluded from transport measurements that the electrical current in lead bromide is carried exclusively by the bromine ions. Therefore, it is not necessary to consider the lattice defects in the lead ion sub-lattice as charge carriers. The crystal structure of lead bromide was determined by Braekken and Harang<sup>3</sup>), and by Nieuwenkamp<sup>4</sup>) and shows a coordination structure formed by a disturbed hexagonal packing of bromine ions between which the lead ions are placed. These lead ions are surrounded by 9 bromine ions at different distances (3.0 to 4.1 Å). In lead bromide the ions at interstitial sites might occur only in the mirror planes (100)<sub>0</sub> and (100)<sub>½</sub>\*, while in the neighbourhood of the gliding mirror planes at (001)<sub>½</sub> and (001)<sub>½</sub>\* bromine ions at 4.1 Å have left enough space for ions with a radius of at most 0.94 Å.

The Pauling radii of bromine and lead ions are 1.95 and 1.21 Å, respectively, so we may disregard the occurrence of interstitial bromine and lead ions and so we consider anion and cation vacancies to be the only intrinsic point defects in lead bromide. According to a Schottky mechanism their thermal generation is given by



where  $V_{\text{Pb}^{2+}}$ ,  $V_{\text{Br}^{-}}$  denote a missing lead ion at a lead ion site and a missing bromine ion at bromine ion site, respectively, and 0 denotes the perfect lattice.

We assume that the foreign ions keep their normal valency states. The electro-neutrality condition upon doping with monovalent cations  $\text{Me}^{+}$ , divalent anions  $\text{A}^{2-}$ , or trivalent cations  $\text{Mc}^{3+}$ , according to the Koch and Wagner system is then given by

$$[V_{\text{Br}^{-}}] + [\text{Mc}^{3+}] = 2[V_{\text{Pb}^{2+}}] + [\text{Me}^{+}] + [\text{A}^{2-}], \quad (4.2)$$

where square brackets denote concentrations. Upon doping with monovalent cations in concentrations well above those of the intrinsic lattice defects this relation becomes

$$[V_{\text{Br}^{-}}] = [\text{Me}^{+}]. \quad (4.3)$$

All foreign ions have radii greater than 0.94 Å, so in all cases the bromine

\*) Values taken from Nieuwenkamp<sup>4</sup>).

ion vacancies are to be considered to carry the electrical current in lead bromide.

With the usual formulas De Vries<sup>1)</sup> derived the temperature and concentration dependence of the ionic conductivity in lead chloride. The same considerations can be used for lead bromide. In the extrinsic conductivity region  $\sigma$  is given by

$$\sigma = B/T \cdot \exp(-U/kT), \quad (4.4)$$

in which  $B$  is a constant. The activation heat  $U$ , for the bromine ion vacancy migration can be obtained from the slopes of the experimental  $\log \sigma T$  versus  $T^{-1}$  curves in the extrinsic conductivity region of the doped crystals. In the intrinsic conductivity region  $\sigma$  is given by

$$\sigma = C/T \cdot \exp(-U/kT) \cdot \exp(-E/3kT), \quad (4.5)$$

in which  $C$  is a constant and  $E$  the heat required for the formation of one set of vacancies ( $V_{\text{Pb}^{2+}} + 2V_{\text{Br}^{-}}$ ). The slope of  $\log \sigma T$  versus  $T^{-1}$  plots in the intrinsic conductivity region gives the value of  $(E/3 + U)$ . Table II gives the values of  $U$  and  $E/3$ , calculated from the measured conductivities of pure and doped crystals.

TABLE II

	Smakula <sup>5)</sup>	authors
Activation heat for $V_{\text{Br}^{-}}$ -migration: $U$	0.28 eV	$0.29 \pm 0.04$ eV
One third of the heat required for the formation of a set of vacancies: $E/3$		$0.48 \pm 0.03$ eV

5. *Some aspects of copper doped crystals.* In section 4 we assume the absence of foreign ions at interstitial sites as the radii of all ions used as dopes are greater than 0.94 Å. However, in the case of copper doped crystals the copper ions may occur at interstitial sites for the Pauling radius of the monovalent copper ion is 0.96 Å. In the extrinsic conductivity region an increase of the conductivity of the copper doped crystals can be seen, the slope of the  $\log \sigma T$  versus  $T^{-1}$  curve in the high temperature region being the same as the curves of lead bromide with monovalent dopants (figure 2). So it is likely that the copper ions occur as monovalent ions at substitutional sites. In the low temperature region a difference in conductivity is observed. The explanation of this behaviour can be that there might occur a segregation of copper bromide after some time. To test this viewpoint two crystals were annealed for 6 hours at 300°C under bromine pressure and in vacuum, respectively. After this treatment the conductivity was measured. This results in both cases in a  $\log \sigma T$  versus  $T^{-1}$  graph with the normal slope in the whole extrinsic conductivity region. With an optical microscope we could not see

a second phase in the copper-doped crystals neither before nor after the annealing procedure. At the low concentrations used the annealing procedure probably dissolves the invisible separated copper (I) bromide again in the crystal.

Crystals with a clearly visible second phase of copper bromide are easily obtained as the latter is not very well soluble in lead bromide. The behaviour of these crystals in conductivity measurements is much the same as the copper-doped crystals not annealed before the measurements.

6. *The photolysis of lead bromide.* After irradiation with ultra violet light lead bromide becomes black<sup>6</sup>). Irradiation in vacuum gives a much higher

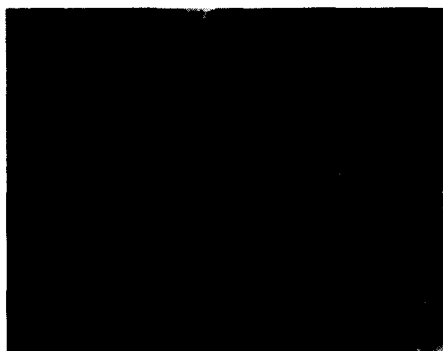


Fig. 4. Electron micrograph of a replica from a cleaved and irradiated lead bromide crystal. Irradiation in air by a high pressure mercury lamp (Philips H.P.K. 125) for 4 hours. Electron microscope: Philips E.M. 200. The micrograph shows a part of the crystal near a step in the (001) surface plane.



Fig. 5. Surface of a cleaved lead bromide crystal irradiated by a high pressure mercury lamp (Philips H.P.K. 125) for 30 minutes through a grid of an electron microscope. A small part of the shadow of this grid can be seen where the crystal was not irradiated. Optical microscope: Reichert Zetopan with interference contrast technique according to Nomarski.

darkening compared with irradiation in air. So vacuum seems a very good halogen acceptor as is the case with the photolysis of the silver halides<sup>7</sup>). A real escape of halogen from the surface is proved by X-ray fluorescence analysis as an irradiated crystal shows an increase in the lead to bromine



0.02mm

Fig. 6. Surface of a cleaved lead bromide crystal irradiated like the crystal of figure 5 but for 2 minutes. Microscope: Reichert Zetopan. Dark field illumination with reflected light.



a-axis

0.02mm

Fig. 7. (001) surface of a cleaved lead bromide crystal etched in a hydrobromic acid-acetone mixture (1 : 1000) for about 1 second. Microscope: Reichert Zetopan with interference contrast technique according to Nomarski.

ratio\*). After prolonged irradiation the surface shows a characteristic damaging as can be made visible by electron microscopy. A cleaved lead bromide crystal was irradiated in air with a high pressure mercury lamp (HPK 125) during four hours. Then the crystal was replicated by first evaporating a film of platinum at an angle of  $60^\circ$  from the normal to the cleavage plane. This was followed by evaporation of a carbon backing layer. The replica was floated off the crystal on an aqueous hydrobromic acid solution and picked up at a screen for observation\*\*). Figure 4 shows a part of the irradiated crystal near a step in the (001) surface plane. Presumably the steep part of this step has not been irradiated as it shows the characteristic appearance of an unirradiated surface.

The result of the photochemical decomposition can be seen as well with an optical microscope at a high magnification. It is most clearly visible with application of the interference contrast technique according to Nomarski as is shown in figure 5. There is a preferential orientation of the photolysis products in the direction of the  $a$  axis. After an irradiation time of a few minutes one can see separate colloidal particles of presumably metallic lead (figure 6). Etching a pure crystal in hydrobromic acid produces oval shaped etch pits lying also in the direction of the  $a$  axis (figure 7).

\*) The authors thank Mr. D. Bax of the "Analytisch Chemisch Laboratorium van de Rijksuniversiteit", Utrecht, for carrying out the analyses.

\*\*\*) The authors thank Mr. J. Pieters of "Centrum voor Submikroskopisch onderzoek van biologische objecten van de Rijksuniversiteit", Utrecht, for this and other electron micrographs.

Together with the electron microscopy results we conclude that the last stage of the photolysis is some kind of photo etching, i.e. the removal of relative large quantities of matter from the surface. This is much the same as the photolysis of lead iodide investigated by Forty and coworkers<sup>8</sup>).

To get more insight into the mechanism of the formation of the lead colloids we did some kinetic measurements. The increase of the optical density was measured as a function of irradiation time. The light of a high pressure mercury lamp (HBO 200) was filtered by an optical reflection interference filter (Schott, R-UV-250) to avoid secondary effects as local

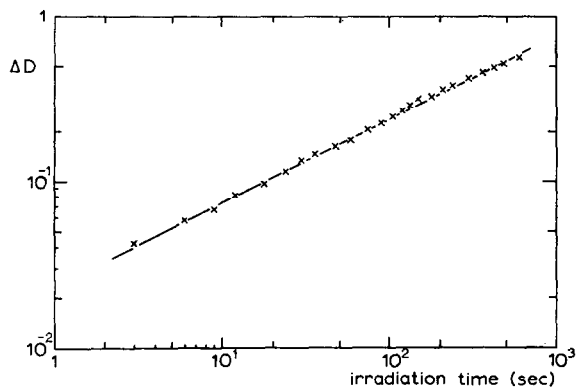


Fig. 8. Change of the optical density  $\Delta D$  of a lead bromide crystal measured parallel to the  $c$ -axis, as a function of irradiation time. Wavelength of the measuring light  $\lambda = 589$  nm.

heating and optical bleaching of the crystal. More details about the experimental set up will be published later. Figure 7 shows the change of the optical density  $\Delta D$  at the wave length  $\lambda = 589$  nm for a cleaved lead bromide crystal irradiated and measured parallel to the  $c$  axis. From this graph it is clear that  $\Delta D$  varies as the square root of the irradiation time. To explain this behaviour it is possible to assume as the rate determining step diffusion through a layer of decomposition products of increasing thickness<sup>8</sup>).

**Acknowledgements.** The authors would like to thank Professor J. H. van Santen for encouraging this work and for many stimulating discussions. The helpful assistance of Mr. G. J. Dirksen during the crystal preparation is gratefully acknowledged.



## REFERENCES

- 1) De Vries, K. J., Thesis Utrecht 1965  
De Vries, K. J. and Van Santen, J. H., *Physica* **29** (1963) 482.
- 2) Tubandt, C. and Eggert, S., *Z. anorg. Chem.* **110** (1920) 196.  
Tubandt, C., *ibid.* **115** (1921) 105.  
Tubandt, C., Reinhold, H. and Liebold, G., *ibid.* **197** (1931) 225.
- 3) Braekken, H. and Harang, L., *Z. Krist.* **68** (1928) 123.
- 4) Nieuwenkamp, W., Thesis Utrecht 1932.
- 5) Smakula, A., M.I.T. Technical Report no. 6 (1965).
- 6) Verwey, J. F., *J. Phys. Chem. Solids* **27** (1966) 468.
- 7) Luckey, W., *J. chem. Phys.* **23** (1955) 882.
- 8) Dawood, R. I., Forty, A. J. and Tubbs, M. R., *Proc. Roy. Soc. A* **284** (1965) 272.